

Finite Difference Method to Solve Incompressible Fluid Flow

NOBUMASA TAKEMITSU

*Mechanical Engineering, Faculty of Engineering, Tokyo Denki University,
2-2 Nishiki-cho, Kanda, Chiyoda-ku, Tokyo, Japan*

Received March 27, 1984; revised February 8, 1985

A method to solve incompressible fluid flow is proposed. The method uses primitive variables (velocity and pressure of the fluid) and introduces an idea that the discretized Navier-Stokes equations have an invariant implicitly in each iteration at any time step. As numerical examples, transient two-dimensional Poiseuille flow and steady flow past a backward-facing step are calculated. It is shown that the method needs fewer iterations than the MAC and the SMAC methods, and the accuracy of the present method is guaranteed by comparison with the analytic solution and the existing methods. © 1985 Academic Press, Inc.

INTRODUCTION

Numerical solutions of Navier-Stokes equations are extremely valuable in studying fluid dynamics. Finite difference methods have been applied (1) where stream function and vorticity are used, and (2) where primitive variables, velocity and pressure, are used. In case (1) the equation of continuity is satisfied exactly by introducing the stream function and convergence is rapid. However, for flows with free surfaces, the boundary conditions present difficulties and, in three dimensions, lack of a scalar stream function inhibits almost the solution [1]. In case (2) boundary conditions and three-dimensional geometry are easily handled. Unfortunately, the velocity components do not automatically satisfy the equation of continuity nor is the convergence rapid [2-9].

This paper presents a new method, using primitive variables, based on the idea of an invariant implicit in each iteration at any time step (unsteady flow), or at any iteration (steady flow). Although applicable to three-dimensional flows, the paper will be restricted to two-dimensional flows.

FORMULATION OF A NEW METHOD

The Navier Stokes equation of a viscous incompressible fluid is expressed in non-dimensional form as

$$\frac{\partial \mathbf{v}}{\partial t} + (\mathbf{v} \cdot \nabla) \mathbf{v} = -\nabla p + \frac{1}{Re} \nabla^2 \mathbf{v}, \quad (1)$$

using a velocity vector \mathbf{v} (Cartesian components u, v, w), time t , pressure p , and the operator nabla ∇ . Here, $Re = UL/\nu$ is the Reynolds number, U the characteristic speed, L the characteristic length of the flow field, and ν the kinematic viscosity of the fluid. The equation of continuity is

$$D = \nabla \cdot \mathbf{v} = 0, \quad (2)$$

where D is dilatation.

When we take the rotation of Eq. (1), the vorticity transport equation

$$\frac{\partial \boldsymbol{\omega}}{\partial t} + (\mathbf{v} \cdot \nabla) \boldsymbol{\omega} - (\boldsymbol{\omega} \cdot \nabla) \mathbf{v} = \frac{1}{Re} \nabla^2 \boldsymbol{\omega} \quad (3)$$

is obtained, where $\boldsymbol{\omega} (= \nabla \times \mathbf{v})$ is vorticity. Velocity is obtained by

$$\mathbf{v} = \nabla \times \boldsymbol{\psi}, \quad \boldsymbol{\omega} = -\nabla^2 \boldsymbol{\psi}. \quad (4a, b)$$

Here, $\boldsymbol{\psi}$ is a stream function, which is a vector potential for three-dimensional flows.

To obtain numerical solutions of Eqs. (1) and (2), or of Eqs. (3) and (4), requires initial and boundary conditions. In both cases, the solution process is iterative. In two-dimensional flows, $\boldsymbol{\psi}$ is a scalar function (see next section) and Eq. (2) is always satisfied exactly. Thus fewer iterations are needed to solve Eqs. (3) and (4) than to solve Eqs. (1) and (2).

Fewer iterations are necessary if some conditions are added implicitly in each iteration when Eqs. (1) and (2) are solved simultaneously. For this purpose add an implicit invariant in each iteration at any time step $t = t$.

When Eqs. (3) and (4) are solved iteratively using the forward-time and centered-space finite difference method at the reference time step $t = t$, the value of the vorticity is unchanged and Eq. (2) is imposed. Moreover, the vorticity remains unchanged when Eqs (1) and (2) are solved iteratively, i.e., the vorticity is invariant at $t = t$. This is expressed as

$$\boldsymbol{\omega}^t = \boldsymbol{\omega}^{(1)} = \boldsymbol{\omega}^{(2)} = \dots = \boldsymbol{\omega}^{(k)} = \boldsymbol{\omega}^{(k+1)} = \dots, \quad (5)$$

where t denotes a time step at $t = t$, and (k) the number of iterations. Hereafter, t is deleted. Equation (5) is rewritten as

$$\boldsymbol{\omega} = \nabla \times \mathbf{v}^{(k)} = \nabla \times \mathbf{v}^{(k+1)}, \quad (6)$$

from which we have

$$\mathbf{v}^{(k+1)} = \mathbf{v}^{(k)} - \nabla \phi^{(k+1)}, \quad (7)$$

where ϕ is a potential function. If we take the divergence of Eq. (7),

$$D^{(k+1)} = D^{(k)} - \nabla^2 \phi^{(k+1)} \quad (8)$$

is obtained. Since the dilatation $D^{(k+1)}$ is zero, we obtain

$$D^{(k)} = \nabla^2 \phi^{(k-1)}. \quad (9)$$

Thus, an invariant is introduced at any time step, if Eq. (9) is solved for ϕ in each iteration. The new velocity field at $k = k + 1$ is obtained from Eq. (7), and the pressure field at $t = t + \Delta t$ ($\Delta t =$ discretized time increment) is obtained from Eq. (1).

In the SMAC (simplified MAC) method [4], the tentative velocities are modified to their final values so as to preserve vorticity at every point. Hence, the basic idea of the SMAC method is that it introduces a tentative velocity field. On the other hand, the present method is based on the idea that the discretized Navier Stokes equation has an invariant in each iteration in the same way as in the stream function and vorticity method. The author believes that the simplest invariant is vorticity. If the vorticity is taken as an invariant, the formulation is somewhat similar to that of the SMAC method except for the calculation of pressure. However, because of the difference of the basic idea between the proposed method and the SMAC method, Eq. (9) plays an important role in the present method, but in the SMAC method the time increment Δt is important. It should also be noted that a potential function ϕ is calculated by

$$\tilde{D} = \nabla^2 \phi \quad (10)$$

in the SMAC method. Here, \tilde{D} is calculated from tentative velocity components, and \tilde{D} remains unchanged until the converged solution is obtained.

This new formulation requires less calculation time than the SMAC method, and the steady-state equation can be evaluated.

NUMERICAL EXAMPLES

A. Unsteady Flow

First, transient two-dimensional Poiseuille flow is studied. The initial and boundary conditions of this flow are

$$t < 0; \quad u = v = \psi = \omega = 0 \quad (\text{everywhere}), \quad (11a)$$

$$t > 0; \quad \psi = \omega = 0 \quad \text{at } y = 0 \text{ (center line)}, \quad (11b)$$

$$\psi = 1, u = \partial\psi/\partial y = 0 \quad \text{at } y = 1 \text{ (upper wall)}, \quad (11c)$$

where u and v are velocity components in x and y directions, respectively, ψ is the scalar stream function, and ω is the vorticity. The analytic solution for this flow, obtained by the Laplace transform, is

$$u = \frac{3}{2}(-y^2 + 1) + \sum_{n=1}^{\infty} \frac{2}{\beta_n^2} \left(\frac{\beta_n \cos \beta_n y}{\sin \beta_n} - 1 \right) \exp(-\beta_n^2 t / Re), \quad (12a)$$

$$v \equiv 0, \quad (12b)$$

$$\psi = \frac{1}{2}(-y^3 + 3y) + \sum_{n=1}^{\infty} \frac{2}{\beta_n^2} \left(\frac{\sin \beta_n y}{\sin \beta_n} - y \right) \exp(-\beta_n^2 t / Re), \quad (12c)$$

$$\omega = 3y + \sum_{n=1}^{\infty} \frac{2 \sin \beta_n y}{\sin \beta_n} \exp(-\beta_n^2 t / Re), \quad (12d)$$

$$\partial p / \partial x = - \left\{ 3 + 2 \sum_{n=1}^{\infty} \exp(-\beta_n^2 t / Re) \right\} / Re, \quad (12e)$$

where β_n is the n th positive solution of $\beta_n = \tan \beta_n$ ($0 < \beta_1 < \beta_2 < \dots$). Numerically, convergence will require, at most, 40 terms in the above series.

In two-dimensional flows, Eqs. (1) and (2) are written in the form

$$\frac{\partial u}{\partial t} + \frac{\partial u^2}{\partial x} + \frac{\partial uv}{\partial y} = -\frac{\partial p}{\partial x} + \frac{1}{Re} \nabla^2 u, \quad (13a)$$

$$\frac{\partial v}{\partial t} + \frac{\partial uv}{\partial x} + \frac{\partial v^2}{\partial y} = -\frac{\partial p}{\partial y} + \frac{1}{Re} \nabla^2 v, \quad (13b)$$

$$D = \frac{\partial u}{\partial x} + \frac{\partial v}{\partial y} = 0. \quad (13c)$$

These equations are discretized as

$$\begin{aligned} u_{i,j}^{t+\Delta t} = & u_{i,j}^t + \Delta t \left[- \left(\frac{u_{i+1/2,j}^2 - u_{i-1/2,j}^2}{h} + \frac{u_{i,j+1/2} v_{i-1/2,j-1} - u_{i,j-1/2} v_{i-1/2,j}}{s} \right) \right. \\ & - \frac{p_{i,j} - p_{i-1,j}}{h} + \frac{1}{Re} \left\{ \frac{1}{h^2} (u_{i+1,j} + u_{i-1,j} - 2u_{i,j}) \right. \\ & \left. \left. + \frac{1}{s^2} (u_{i,j+1} + u_{i,j-1} - 2u_{i,j}) \right\} \right], \end{aligned} \quad (14a)$$

$$\begin{aligned} v_{i,j}^{t+\Delta t} = & v_{i,j}^t + \Delta t \left[- \left(\frac{u_{i+1,j-1/2} v_{i+1/2,j-1/2} - u_{i,j-1/2} v_{i-1/2,j-1/2}}{h} + \frac{v_{i,j+1/2}^2 - v_{i,j-1/2}^2}{s} \right) \right. \\ & - \frac{p_{i,j} - p_{i,j-1}}{s} + \frac{1}{Re} \left\{ \frac{1}{h^2} (v_{i+1,j} + v_{i-1,j} - 2v_{i,j}) \right. \\ & \left. \left. + \frac{1}{s^2} (v_{i,j+1} + v_{i,j-1} - 2v_{i,j}) \right\} \right], \end{aligned} \quad (14b)$$

$$D_{i,j} = \frac{u_{i+1,j} - u_{i,j}}{h} + \frac{v_{i,j+1} - v_{i,j}}{s}. \quad (14c)$$

The indices i and j count cell-center, cell-boundary, or cell-corner positions in the x and y directions, and h and s are mesh sizes in the x and y directions, respectively. The superscript indices t and $t + \Delta t$ ($\Delta t =$ time increment) show time steps. The velocity components u and v are defined at cell boundaries; pressure p and dilatation D are defined at cell centers; the stream function ψ and the vorticity ω are defined at cell corners (see Fig. 1). The quantities at all fractional indices are obtained as simple averages of the two adjacent quantities, e.g.,

$$u_{i+1/2,j} = (u_{i,j} + u_{i+1,j})/2, \quad \text{etc.}$$

Equations (3) and (4) become

$$\frac{\partial \omega}{\partial t} + \frac{\partial u \omega}{\partial x} + \frac{\partial v \omega}{\partial y} = \frac{1}{Re} \nabla^2 \omega, \tag{15a}$$

$$\omega = -\nabla^2 \psi, \quad u = \partial \psi / \partial y, \quad v = -\partial \psi / \partial x \tag{15b. c}$$

in the two-dimensional case (ψ - ω method). These equations are discretized as

$$\begin{aligned} \omega_{i,j}^{t+\Delta t} = \omega_{i,j}^t + \Delta t \left[- \left(\frac{u_{i+1,j-1/2} \omega_{i+1,j} - u_{i-1,j-1/2} \omega_{i-1,j}}{2h} \right. \right. \\ \left. \left. + \frac{v_{i-1/2,j+1} \omega_{i,j+1} - v_{i-1/2,j-1} \omega_{i,j-1}}{2s} \right) + \frac{1}{Re} \left\{ \frac{1}{h^2} (\omega_{i+1,j} \right. \right. \\ \left. \left. + \omega_{i-1,j} - 2\omega_{i,j}) + \frac{1}{s^2} (\omega_{i,j+1} + \omega_{i,j-1} - 2\omega_{i,j}) \right\} \right]^t, \end{aligned} \tag{16a}$$

$$2 \left(\frac{1}{h^2} + \frac{1}{s^2} \right) \psi_{i,j}^* = \frac{1}{h^2} (\psi_{i+1,j} + \psi_{i-1,j}) + \frac{1}{s^2} (\psi_{i,j+1} + \psi_{i,j-1}) + \omega_{i,j}, \tag{16b}$$

$$\psi_{i,j}^{(k+1)} = \psi_{i,j}^{(k)} + \text{RF}_{\psi} (\psi_{i,j}^* - \psi_{i,j}^{(k)}). \tag{16c}$$

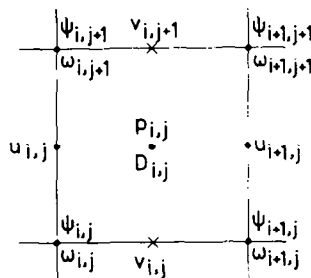


FIG. 1. Placement of field variables.

Here, we introduce a relaxation factor RF_ψ for ψ . Velocity components $u_{i,j}$ and $v_{i,j}$ are calculated from

$$u_{i,j} = (\psi_{i,j+1} - \psi_{i,j})/s, \quad v_{i,j} = -(\psi_{i+1,j} - \psi_{i,j})/h. \quad (16d)$$

Solutions are obtained by four methods; the ψ - ω method, the MAC method, the SMAC method, and the present method.

In the MAC method, the pressure field is obtained by solving

$$2 \left(\frac{1}{h^2} + \frac{1}{s^2} \right) p_{i,j}^* = \frac{1}{h^2} (p_{i+1,j} + p_{i-1,j}) + \frac{1}{s^2} (p_{i,j+1} + p_{i,j-1}) + \left\{ -\frac{D_{i,j}}{\Delta t} + \frac{\hat{c}^2 u^2}{\hat{c} x^2} + 2 \frac{\partial^2 uv}{\partial x \partial y} + \frac{\hat{c}^2 v^2}{\hat{c} y^2} - \frac{1}{\text{Re}} \nabla^2 D \right\}', \quad (17a)$$

$$p_{i,j}^{(k+1)} = p_{i,j}^{(k)} + \text{RF}_p (p_{i,j}^* - p_{i,j}^{(k)}), \quad (17b)$$

where RF_p is a relaxation factor for p .

In the SMAC method, the tentative velocity $\tilde{\mathbf{v}}(\tilde{u}, \tilde{v})$ is calculated from

$$\tilde{\mathbf{v}} = \mathbf{v}' + \Delta t \left[-(\mathbf{v} \cdot \nabla \mathbf{v}) - \nabla p + \frac{1}{\text{Re}} \nabla^2 \mathbf{v} \right]', \quad (18a)$$

$$\tilde{D} = \nabla \cdot \tilde{\mathbf{v}}, \quad (18b)$$

and velocity components at $t = t + \Delta t$ are corrected by

$$2 \left(\frac{1}{h^2} + \frac{1}{s^2} \right) \phi_{i,j}^* = \frac{1}{h^2} (\phi_{i+1,j} + \phi_{i-1,j}) + \frac{1}{s^2} (\phi_{i,j+1} + \phi_{i,j-1}) - \tilde{D}_{i,j}, \quad (18c)$$

$$\phi_{i,j}^{(k+1)} = \phi_{i,j}^{(k)} + \text{RF}_\phi (\phi_{i,j}^* - \phi_{i,j}^{(k)}), \quad (18d)$$

$$\mathbf{v}^{t+\Delta t} = \tilde{\mathbf{v}} - \nabla \phi, \quad (18e)$$

where RF_ϕ is a relaxation factor for ϕ .

In the present method, $\mathbf{v}^{t+\Delta t}$ is calculated from Eqs. (14a), (14b), and $\mathbf{v}^{t+\Delta t}$ is corrected by

$$D^{(k)} = \nabla \cdot \mathbf{v}^{(k)}, \quad (19a)$$

$$2 \left(\frac{1}{h^2} + \frac{1}{s^2} \right) \phi_{i,j}^* = \frac{1}{h^2} (\phi_{i+1,j} + \phi_{i-1,j}) + \frac{1}{s^2} (\phi_{i,j+1} + \phi_{i,j-1}) - D_{i,j}^{(k)}, \quad (19b)$$

$$\phi_{i,j}^{(k+1)} = \phi_{i,j}^{(k)} + \text{RF}_\phi (\phi_{i,j}^* - \phi_{i,j}^{(k)}), \quad (19c)$$

$$\mathbf{v}^{t+\Delta t(k+1)} = \mathbf{v}^{t+\Delta t(k)} - \nabla \phi^{(k+1)}, \quad (19d)$$

where RF_ϕ is a relaxation factor for ϕ .

Let $Re = 5$ and divide the flow field as shown in Fig. 2. Mesh sizes h and s are $h = s = 0.1$, and $IC = 61$, $JC = 13$, and the time increment $\Delta t = 1/100$.

The initial values for u , v , p , ψ , and ω are all equal to zero, and the boundary conditions are:

(a) Upstream boundary

- (1) u, ψ, ω : given by the analytic solution,
- (2) $v = 0$,
- (3) $p = 0$,
- (4) $\phi_{i-1,j} = \phi_{i,j}$ ($i = 2$).

(b) Upper wall

- (1) ψ : given by the analytic solution,
- (2) $\omega_{i,j}$: calculated by $2(\psi_{i,j} - \psi_{i,j-1})/s^2$ ($j = JC - 1$),
- (3) $u_{i,j+1} = -u_{i,j}$ ($j = JC - 2$),
- (4) $v = 0$,
- (5) $p_{i,j+1} = p_{i,j} + (2/sRe)(v_{i,j} - v_{i,j-1})$, where $v_{i,j+2} = v_{i,j}$ and $D_{i,j+1} = D_{i,j}$ ($j = JC - 2$, MAC method),
- (6) $\phi_{i,j+1} = \phi_{i,j}$ ($j = JC - 2$).

(c) Lower boundary (center line)

- (1) $\psi = \omega = 0$,
- (2) $u_{i,j-1} = u_{i,j}$ ($j = 2$),
- (3) $v = 0$,
- (4) $\phi_{i,j-1} = \phi_{i,j}$ ($j = 2$),
- (5) $p_{i,j-1} = p_{i,j}$ ($j = 2$, MAC method),
- (6) $v_{i,j-1} = -v_{i,j+1}$ ($j = 2$, MAC method).

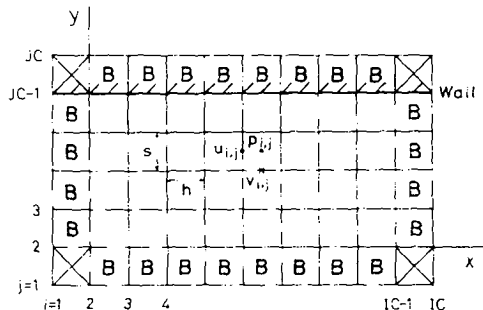


FIG. 2. Discretion of the flow field. B-- boundary cell, open box -- fluid cell.

(d) Downstream boundary

- (1) $\partial^2\psi/\partial x^2 = 0$,
- (2) $\partial\omega/\partial x = 0$,
- (3) $\partial v/\partial x = 0$,
- (4) $u_{i+1,j} = u_{i,j} - (h/s)(v_{i,j+1} - v_{i,j})$ ($i = IC - 1$),
- (5) $\phi = 0$,
- (6) $\partial^2 p/\partial x^2 = 0$ (MAC method).

In the SMAC and the present method if the condition

$$\phi_{i-1,j} = \phi_{i,j}$$

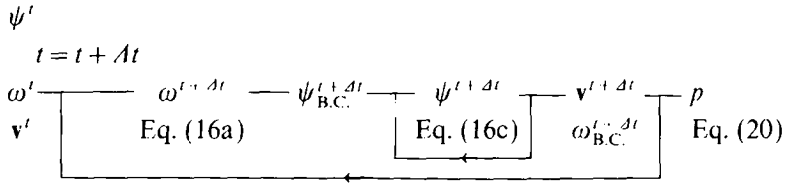
is imposed at the upstream end, then

$$\left(\frac{1}{h^2} + \frac{2}{s^2}\right)\phi_{i,j}^* = \frac{\phi_{i+1,j}}{h^2} + \frac{1}{s^2}(\phi_{i,j+1} + \phi_{i,j-1}) - D_{i,j}$$

is used instead of Eqs. (18c) or (19b).

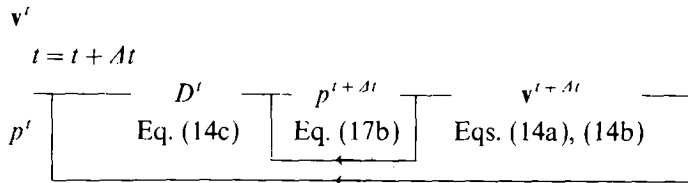
The numerical procedures per cycle are:

(i) ψ - ω method

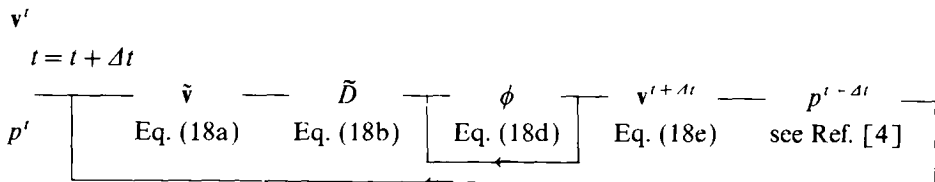


where suffix B.C. denotes boundary conditions.

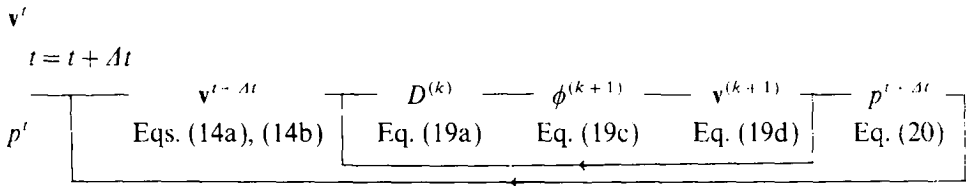
(ii) MAC method



(iii) SMAC method



(iv) Present method



The main calculations proceed from left to right, and the notation \leftarrow denotes iterations. In the above numerical procedures, Eqs. (16b), (17a), (18c), and (19b) are all solved by the SLOR method [10], the relaxation factors are $\text{RF}_\psi = \text{RF}_p = \text{RF}_\phi = 1.8$ in the ψ - ω method, the MAC method, and the SMAC method, and $\text{RF}_\phi = 1$ in the present method. In the ψ - ω method and the present method, the pressure field at new time step is calculated by

$$(\nabla p)^{t+\Delta t} = -\left(\frac{\partial \mathbf{v}}{\partial t}\right)' - \nabla \cdot (\mathbf{v}\mathbf{v})' + \frac{1}{\text{Re}} (\nabla^2 \mathbf{v})', \quad (20)$$

where $(\partial \mathbf{v} / \partial t)'$ is evaluated by simple forward differences. In this problem, pressure is integrated from left to right at $y = 1 - s/2$ and from top to bottom at x .

Figure 3 shows the convergence rate by various methods. In the figure, ε_f is defined by

$$\varepsilon_f = |f_{i,j}^{(k)} - f_{i,j}^{(k-1)}|_{\max}, \quad (21)$$

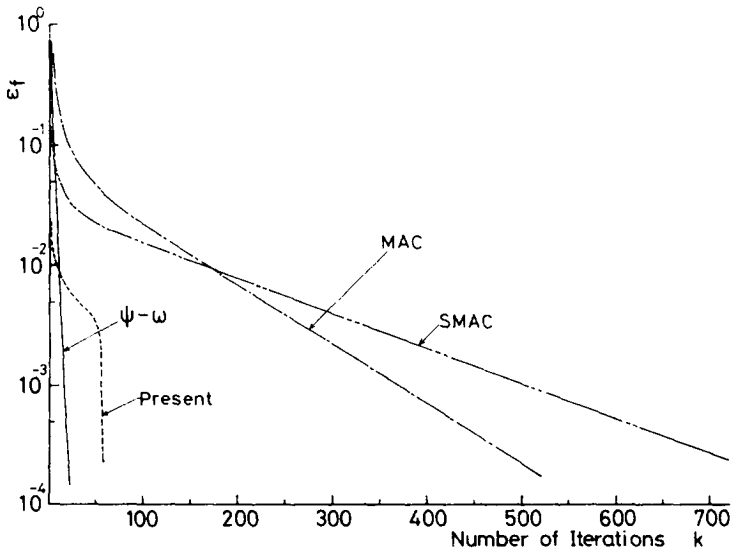


FIG. 3. Typical demeanor of convergence by various methods.

where $|\cdot|_{\max}$ denotes maximum value of $|\cdot|$, and f stands for ψ (ψ - ω method), p (MAC method), or ϕ (SMAC and the present method).

The velocity profiles at $t=2\Delta t$ are shown in Fig. 4. Only the solution by the MAC method is quite different from the analytic solution. The MAC method represents fluid driven by a pressure gradient (see Eq. (17a)). Therefore, when the fluid starts impulsively from rest to a finite velocity, the solution by the MAC method is not accurate in the whole flow field. In the MAC method, maximum error of dilatation ε_D was 10.5, where ε_D is defined by

$$\varepsilon_D = |D_{i,j}|_{\max}. \quad (22)$$

The solution by the SMAC method, while accurate ($\varepsilon_D = 1.1 \times 10^{-2}$), required many iterations to obtain convergence (see Fig. 3). The solutions by the present method are very close to the analytic solution. When we stop iterations with the condition that ε_D is $O(10^{-2})$, the velocity profile is very close to the one by the ψ - ω method, and if we stop iterations when ε_D is $O(10^{-3})$, the solution agrees almost precisely with the solution by the ψ - ω method.

However, the convergent process is not easy to analyze and is not always stable in the present method. Therefore ϕ is set to zero when $\varepsilon_D^{(k)}$ becomes larger than $\varepsilon_D^{(k-1)}$, or when $\varepsilon_D^{(k)}$ becomes larger than $\varepsilon_D^{(k-1)}$ and $\varepsilon_\phi^{(k)}$ becomes larger than $\varepsilon_\phi^{(k-1)}$. In this problem, previous values of ϕ are used ($\varepsilon_D < 10^{-2}$), or ϕ is set equal to zero, when $\varepsilon_D^{(k)}$ becomes larger than $\varepsilon_D^{(k-1)}$ ($\varepsilon_D < 5 \times 10^{-3}$). (See also Section B, Steady Flow.)

Figure 5 shows velocity profiles by the four methods at $t=0.5$ (at downstream end). Again only the solution by the MAC method is not close to the analytic solution. More time steps are necessary to make ε_D small; ε_D is still 5.2 in the MAC method.

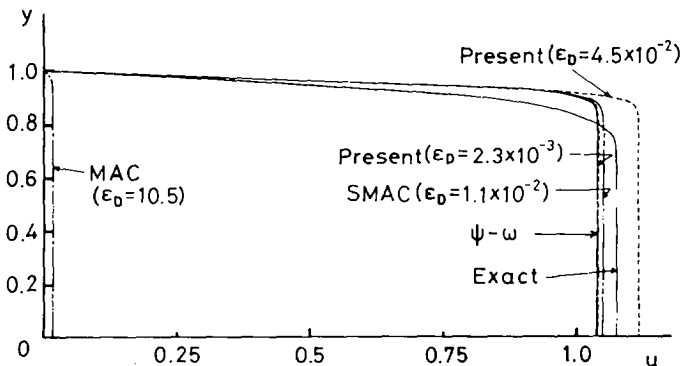


FIG. 4. Velocity profiles by various methods at downstream end ($t=0.02$).

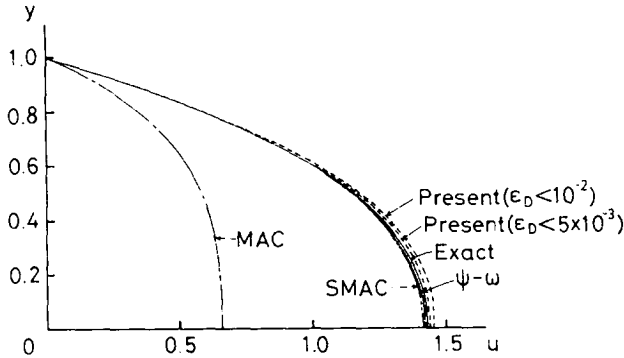


FIG. 5. Velocity profiles by various methods at down stream end ($t = 0.5$).

In Fig. 6, global error of convective terms, defined by

$$\epsilon_g = \sum_{\substack{i=3,JC-2 \\ j=2,JC-2}} \left(\left| \frac{\partial u^2}{\partial x} \right| + \left| \frac{\partial uw}{\partial y} \right| \right) + \sum_{\substack{i=2,JC-2 \\ j=3,JC-2}} \left(\left| \frac{\partial wv}{\partial x} \right| + \left| \frac{\partial v^2}{\partial y} \right| \right), \quad (23)$$

is shown. The error by the ψ - ω method, the SMAC method, and the present method decreases as time increases. The magnitude of the error by the SMAC method is the same as that of the ψ - ω method. Although ϵ_g is shown increasing with time in the MAC method, it will eventually decrease.

Figure 7a shows the pressure distribution along the center line at $t = 0.5$. Only the MAC method is quite different from the analytic solution.

Figures 4, 5, 6, and 7a indicate that the SMAC method is more accurate than the present method since ϵ_g is small. However, this is not true in general. Figure 7b

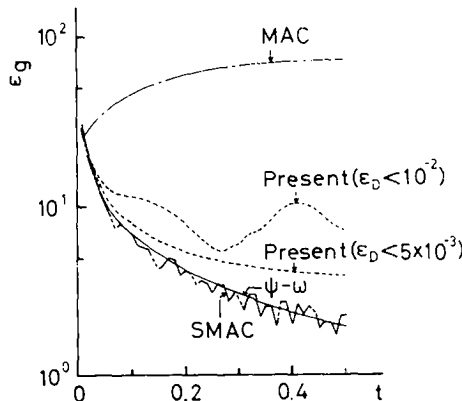


FIG. 6. Temporal global error ϵ_g by various methods.

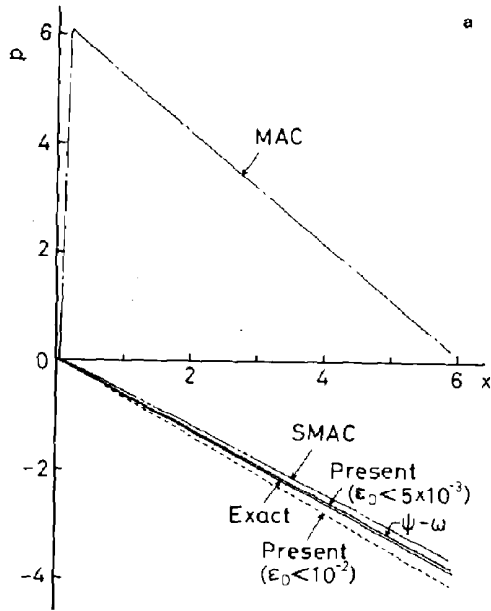


FIG. 7a. Pressure distributions by various methods along center line ($t = 0.5$).

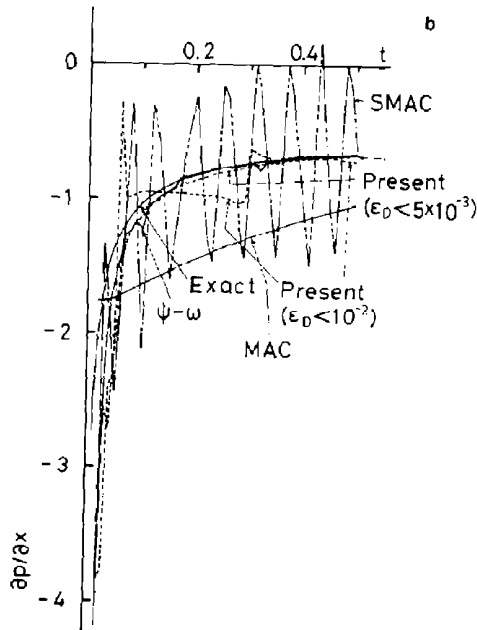


FIG. 7b. Temporal pressure gradient at $x = 3$ on center line by various methods.

TABLE I
Comparison of the Number of Iterations by Various Methods

Methods	Criterion of convergence	Number of iterations	CPU time (approx.) (sec)
$\psi-\omega$	$\varepsilon_\omega < 2.0 \times 10^{-4}$	232	4
MAC	$\varepsilon_p < 2.0 \times 10^{-4}$	6678	34
SMAC	$\varepsilon_\phi < 2.0 \times 10^{-4}$	5869	26
Present	$\varepsilon_D < 1.0 \times 10^{-2}$	314	5
	$\varepsilon_D < 5.0 \times 10^{-3}$	506	6

shows temporal pressure gradients at $x = 3$ on center line by various methods. Only in the present method, with $\varepsilon_D < 5 \times 10^{-3}$, and in the $\psi-\omega$ method is the pressure gradient calculated accurately even for small time values. The SMAC method shows severe oscillation, and the MAC method is inaccurate (see also Fig. 7a).

Table I shows number of iterations and CPU times by various methods. The solution by the $\psi-\omega$ method is very fast and is accurate. The number of iterations required for convergence by the present method is about 1.5 times that by the $\psi-\omega$ method, and about 1/20 times smaller compared with the MAC and the SMAC methods. Moreover, the solutions by the present method are accurate.

B. Steady Flow

As a simple example which has a corner in fluid, a steady flow past a backward-facing step is studied (see Fig. 8).

In steady flow problems, the Navier-Stokes equations are written in the form

$$\frac{\partial u^2}{\partial x} + \frac{\partial uv}{\partial y} = -\frac{\partial p}{\partial x} + \frac{1}{Re} \nabla^2 u, \quad (24a)$$

$$\frac{\partial uv}{\partial x} + \frac{\partial v^2}{\partial y} = -\frac{\partial p}{\partial y} + \frac{1}{Re} \nabla^2 v, \quad (24b)$$

$$D = \frac{\partial u}{\partial x} + \frac{\partial v}{\partial y} = 0, \quad (24c)$$

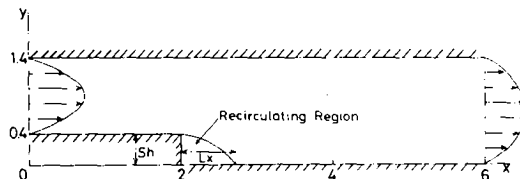


FIG. 8. Backward-facing step flow.

and

$$\frac{\partial u \omega}{\partial x} + \frac{\partial v \omega}{\partial y} = \frac{1}{Re} \nabla^2 \omega, \quad (25a)$$

$$\omega = -\nabla^2 \psi, \quad u = \partial \psi / \partial y, \quad v = -\partial \psi / \partial x. \quad (25b, c)$$

Since the iterative solution of vorticity often diverges at higher Reynolds numbers, methods to stabilize the calculation of vorticity should be used. In the present calculation, the author's method [11] is modified so that the vorticity obtained from Eq. (25) is the same as that obtained from Eqs. (24). This method has second-order accuracy in the whole flow field and avoids iteration divergence. Similar stabilized finite difference equations, which are different from second-order upstream difference equations (see, for examples, Ref. [12]), have been previously published [13-15]. In this problem we use the finite difference equations

$$\begin{aligned} & \left\{ \frac{2}{Re} \left(\frac{1}{h^2} + \frac{1}{s^2} \right) + \mu \left(\frac{1}{h} + \frac{1}{s} \right) \right\} u_{i,j}^* \\ &= - \left(\frac{u_{i+1/2,j}^2 - u_{i-1/2,j}^2}{h} + \frac{u_{i,j+1/2} v_{i-1/2,j+1} - u_{i,j-1/2} v_{i-1/2,j}}{s} \right) + \mu \left(\frac{1}{h} + \frac{1}{s} \right) u_{i,j} \\ & \quad - \frac{p_{i,j} - p_{i-1,j}}{h} + \frac{1}{Re} \left\{ \frac{1}{h^2} (u_{i+1,j} + u_{i-1,j}) + \frac{1}{s^2} (u_{i,j+1} + u_{i,j-1}) \right\}, \end{aligned} \quad (26a)$$

$$u_{i,j}^{(k+1)} = u_{i,j}^{(k)} + RF_u (u_{i,j}^* - u_{i,j}^{(k)}), \quad (26b)$$

and

$$\begin{aligned} & \left\{ \frac{2}{Re} \left(\frac{1}{h^2} + \frac{1}{s^2} \right) + \mu \left(\frac{1}{h} + \frac{1}{s} \right) \right\} v_{i,j}^* \\ &= - \left(\frac{u_{i+1,j-1/2} v_{i+1/2,j} - u_{i,j-1/2} v_{i-1/2,j}}{h} + \frac{v_{i,j+1/2}^2 - v_{i,j-1/2}^2}{s} \right) + \mu \left(\frac{1}{h} + \frac{1}{s} \right) v_{i,j} \\ & \quad - \frac{p_{i,j} - p_{i,j-1}}{s} + \frac{1}{Re} \left\{ \frac{1}{h^2} (v_{i+1,j} + v_{i-1,j}) + \frac{1}{s^2} (v_{i,j+1} + v_{i,j-1}) \right\}, \end{aligned} \quad (26c)$$

$$v_{i,j}^{(k+1)} = v_{i,j}^{(k)} + RF_v (v_{i,j}^* - v_{i,j}^{(k)}), \quad (26d)$$

$$D_{i,j}^{(k+1)} = \left(\frac{u_{i+1,j} - u_{i,j}}{h} + \frac{v_{i,j+1} - v_{i,j}}{s} \right)^{(k+1)}, \quad (26e)$$

where μ , a relation factor, stabilizes the iterative process, and RF_u and RF_v are relaxation factors for u and v , respectively (present method).

In the ψ - ω method, Eq. (25) is discretized as

$$\left\{ \frac{2}{Re} \left(\frac{1}{h^2} + \frac{1}{s^2} \right) + \frac{\mu}{2} \left(\frac{1}{h} + \frac{1}{s} \right) \right\} \omega_{i,j}^* \\ = - \left(\frac{u_{i+1,j} - 1/2\omega_{i+1,j} - u_{i-1,j} - 1/2\omega_{i-1,j}}{2h} + \frac{v_{i,1/2,j+1}\omega_{i,j+1} - v_{i,1/2,j-1}\omega_{i,j-1}}{2s} \right) \\ + \frac{\mu}{2} \left(\frac{1}{h} + \frac{1}{s} \right) \omega_{i,j} + \frac{1}{Re} \left\{ \frac{1}{h^2} (\omega_{i+1,j} + \omega_{i-1,j}) + \frac{1}{s^2} (\omega_{i,j+1} + \omega_{i,j-1}) \right\}, \quad (27a)$$

$$\omega_{i,j}^{(k+1)} = \omega_{i,j}^{(k)} + \text{RF}_\omega (\omega_{i,j}^* - \omega_{i,j}^{(k)}), \quad (27b)$$

where RF_ω is a relaxation factor for ω .

The case of $Re = 50$ is studied and mesh sizes h and s are chosen as $h = s = 0.1$. As is shown in Fig. 8, the length of the channel is taken as 6, and the height as 1.4, and the backward-facing step is located at $x = 2$ and its height Sh is 0.4, and L_x denotes the length of recirculating region.

Initial values are set equal to those from steady Poiseuille flow,

$$u = -6y^2 + 6(2y_1 + 1)y - 6y_1(y_1 + 1), \quad v \equiv 0, \quad (28a)$$

$$\psi = -2y^3 + 3(2y_1 + 1)y^2 - 6y_1(y_1 + 1)y + y_1^2(2y_1 + 3), \quad (28b)$$

$$\omega = 12y - 6(2y_1 + 1), \quad (28c)$$

where $y_1 = 0.4$. Pressure equals zero in the whole flow field. Boundary conditions are imposed at the upstream end in the same form as Eqs. (28a), (28b), (28c):

$$u_{i,j-1} = -u_{i,j} \quad (j=2) \quad \text{or} \quad u_{i,j-1} = -u_{i,j} \quad (j=JC-2), \\ v = 0, \quad (28d)$$

$$\psi = 0 \quad \text{or} \quad \psi = 1 \quad (28e)$$

on the wall.

In the present method, ϕ is calculated by the equations

$$(2/h^2 + 1/s^2) \phi_{i,j}^* = (\phi_{i+1,j} + \phi_{i-1,j})/h^2 + \phi_{i,j-1}/s^2 - D_{i,j}^{(k)}, \quad (29a)$$

$$(1/h^2 + 2/s^2) \phi_{i,j}^* = \phi_{i+1,j}/h^2 + (\phi_{i,j-1} + \phi_{i,j-2})/s^2 - D_{i,j}^{(k)}, \quad (29b)$$

instead of Eq. (19b) at the corner C , since ϕ is a multi-valued function (see Fig. 9).

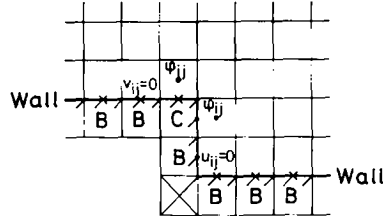
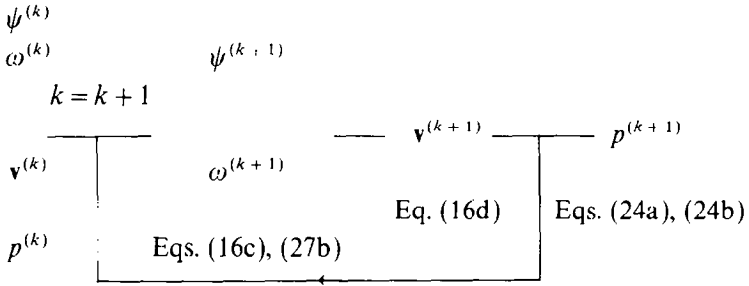


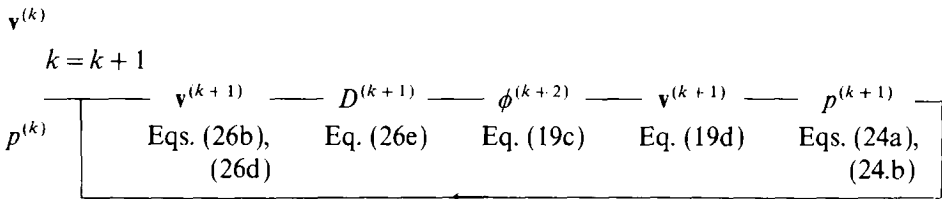
FIG. 9. Corner cell. B = Boudary cell, C = corner cell, open box = fluid cell.

Two calculation procedures follow:

(i) ψ - ω method



(ii) Present method



The relaxation factors RF_ψ , RF_ω , RF_u , RF_v , and μ are all taken to be 1.

Table II shows the comparison of number of iterations and errors ϵ_f ($f \equiv \psi, \omega, u, v$), ϵ_D (Eq. (22)), and ϵ_M which is defined by

$$\epsilon_M = |\text{left-hand side of Eqs. (24a), (24b)} - \text{right-hand side of Eqs. (24a), (24b)}|_{\max},$$

or

$$= |\text{left-hand side of Eq. (25a)} - \text{right-hand side of Eq. (25a)}|_{\max}.$$

TABLE II
 Comparison of the Number of Iterations, Errors ϵ_f ($f = \psi, \omega$ or u, v),
 ϵ_D , and ϵ_M , and Vortex Length L_v by Various Methods

Methods	Number of Iterations	ϵ_f	ϵ_D	ϵ_M	L_v	Comments
ψ						
ω	328	1.979×10^{-4}		2.169×10^{-3}	0.765	
	1832	2.665×10^{-3}		3.328×10^{-3}	0.770	
Present I	600	3.363×10^{-4}	7.915×10^{-2}	3.576×10^{-3}	0.580	Time-marching method (500 steps) $\phi = 0$ in each iteration
II	553	4.718×10^{-4}	9.938×10^{-3}	6.287×10^{-3}	0.746	If $\epsilon_D^{(k)} > \epsilon_B^{(k-1)}$, $\phi = 0$
III	347	2.884×10^{-3}	9.875×10^{-3}	3.885×10^{-2}	0.724	If $\epsilon_D^{(k)} > \epsilon_B^{(k-1)}$ and $\epsilon_\psi^{(k)} > \epsilon_\psi^{(k-1)}$, $\phi = 0$

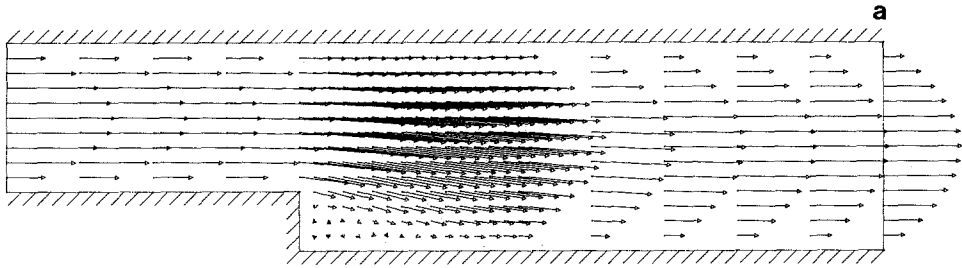


FIG. 10a. Velocity vectors obtained by the present method III. Unit velocity vector = \rightarrow .

The ψ - ω method is the fastest one to obtain a solution in steady flow. But the time-marching method by the ψ - ω method (calculated by Eqs. (16a), (16c) and $\Delta t = 1/100$) needs more time to obtain a converged solution, because ε_ω is larger by one order compared with the ψ - ω method (see also Fig. 11). Too many iterations are needed to obtain convergence in the present method I, where $\phi = 0$ in each iteration; but the iteration process is the most stable. If we put $\phi = 0$ when $\varepsilon_D^{(k)} > \varepsilon_D^{(k-1)}$ (present method II), the iteration process is less stable but ε_D is smaller by one order compared with the present method I with almost the same iteration number. If we put $\phi = 0$ when $\varepsilon_D^{(k)} > \varepsilon_D^{(k-1)}$ and $\varepsilon_\phi^{(k)} > \varepsilon_\phi^{(k-1)}$ (present method III), the number of iterations is almost the same as that by the ψ - ω method, and the solution obtained is accurate if the iteration process remains stable.

Velocity vectors and stream functions obtained by the present method III are shown in Figs. 10a and b, respectively.

Figure 11 shows vorticity distributions on the wall by various methods. Solution by the time-marching method has not yet converged in steady state because the absolute values of the vorticity on the wall at the downstream end are not nearly equal. Solution by the present method III is very close to the one by the ψ - ω method.

From the table and figures, it is considered that the present method is accurate and needs less time to obtain solution for steady flow, too.

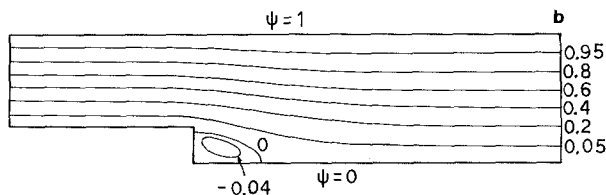


FIG. 10b. Streamlines obtained by the present method III.

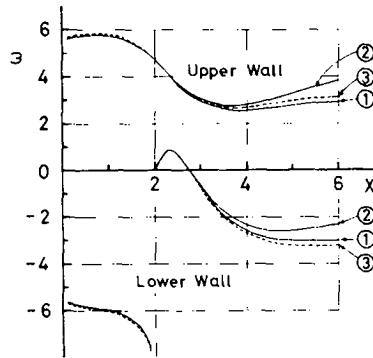


FIG. 11. Vorticity distributions on the wall obtained by various methods. 1 = $\psi - \omega$, 2 = $\psi - \omega$ (time-marching method), 3 = present method III.

CONCLUSIONS

A new method, in which an idea that the Navier-Stokes equations have an invariant implicitly in each iteration at any time step or at any iteration is applied, is presented. Using this method, some numerical experiments were performed. As a result of this study, we conclude:

- (1) Navier-Stokes equations with an invariant implicitly in each iteration produce efficient and accurate numerical solutions.
- (2) The proposed method is also applicable to steady flow and three-dimensional flow problems.

The method proposed here has also been extended to the Crank-Nicolson method, a non-iterative implicit method, and a two-step method [16].

ACKNOWLEDGMENTS

The author wishes to express his sincere gratitude to Professor M. Kawaguti and Prof. Y. Matunobu of Keio University, and to Professor S. Mizuki and assistant engineer N. Shinya of Hosei University. Examples of unsteady flow were calculated by FACOM M-380R at Keio University and the steady flows were calculated by ACOS 6 computer at Hosei University.

REFERENCES

1. A. THOM, *Proc. R. Soc. London, Ser. A.* **141** (1933), 651.
2. F. H. HARLOW AND J. E. WELCH, *Phys. Fluids* **8** (1965), 2182; J. E. WELCH, F. H. HARLOW, J. P. SHANNON, AND B. J. DALY, Los Alamos Scientific Report LA-3425, 1966.
3. A. J. CHORIN, *Math. Comp.* **22** (1968), 745.
4. A. A. AMSDEN AND F. H. HARLOW, Los Alamos Scientific Report LA-4370, 1970.

5. W. E. PRACHT, *J. Comput. Phys.* **7** (1971), 46.
6. J. E. VIECELLI, *J. Comput. Phys.* **8** (1971), 119.
7. H. TAKAMI AND K. KUWAHARA, *J. Phys. Soc. Jpn.* **37** (1974), 1695.
8. C. W. HIRT, B. D. NICHOLS, AND N. C. ROMERO, Los Alamos Scientific Report LA-5852, 1975.
9. C. W. HIRT AND B. D. NICHOLS, *J. Comput. Phys.* **34** (1980), 390.
10. R. S. VARGA, "Matrix Iterative Analysis," p. 199, Prentice-Hall, Englewood Cliffs, N.J., 1962.
11. N. TAKEMITSU, *J. Comput. Phys.* **36** (1980), 236.
12. B. P. LEONARD, in "Computer Methods in Fluids" (K. Morgan, C. Taylor, and C. A. Brebbia, Eds.), p. 159, Pentech Press, London/Plymouth, 1980.
13. S. C. R. DENNIS AND G.-Z. CHANG, *Phys. Fluids, Suppl. II*, (1969), 88.
14. S. OZAWA, *J. Phys. Soc. Jpn.* **38** (1975), 889.
15. H. FASEL, in "Computational Fluid Dynamics" (W. Kollman, Ed.), p. 167, Hemisphere Publishing Corporation, Washington/New York/London, 1980.
16. N. TAKEMITSU, submitted for publication.